Lepton flavor violating dark photon

Alexey S. Zhevlakov,[1,2,*] Dmitry V. Kirpichnikov,[3,†] and Valery E. Lyubovitskij[4,5,6,‡]

[1]Bogoliubov Laboratory of Theoretical Physics, JINR, 141980 Dubna, Russia
[2]Matrosov Institute for System Dynamics and Control Theory SB RAS, Lermontov str., 134, 664033, Irkutsk, Russia
[3]Institute for Nuclear Research of the Russian Academy of Sciences, 117312 Moscow, Russia
[4]Institut für Theoretische Physik, Universität Tübingen, Kepler Center for Astro and Particle Physics, Auf der Morgenstelle 14, D-72076 Tübingen, Germany
[5]Departamento de Física y Centro Científico Tecnológico de Valparaíso-CCTVal, Universidad Técnica Federico Santa María, Casilla 110-V, Valparaíso, Chile
[6]Millennium Institute for Subatomic Physics at the High-Energy Frontier (SAPHIR) of ANID, Fernández Concha 700, Santiago, Chile

(Received 28 July 2023; accepted 19 December 2023; published 16 January 2024)

We study the possible impact of dark photons on lepton flavor phenomenology. We derive the constraints on nondiagonal dark photon couplings with leptons by analyzing corresponding contributions to lepton anomalous magnetic moments, rare lepton decays, and the prospects of fixed-target experiments aimed at searching for light dark matter based on missing energy/momentum techniques.

DOI: 10.1103/PhysRevD.109.015015

I. INTRODUCTION

The direct search for dark matter (DM) remains one of the most challenging issues in particle physics. Astrophysical data and cosmological observations at different scales indirectly imply the existence of DM. Despite numerous intensive direct searches for DM in accelerator-based experiments, little is known about the origin and dynamics of weakly coupled particles of the hidden sector. In addition, the muon $(g-2)$ anomaly [1] and recent tensions between Standard Model (SM) expectations and experimental measurements [2–5] has stimulated the development of various beyond-the-SM (BSM) scenarios involving sub-GeV hidden sector particles [6].

Typically, such scenarios imply feebly interacting mediator (portal) states connecting the BSM sector with SM particles. In particular, several such hidden-sector scenarios were recently discussed in the literature: the Higgs portal [7–9], tensor portal [10–12], dark photon portal [13–15], sterile neutrino portal [16], axion portal [17], and Stueckelberg portal [15,18].

It is worth noticing that some hidden-sector models suggest an idea of lepton nonuniversality and lepton flavor violation (LFV). In this sense, a light sub-GeV hidden particle may potentially explain the muon $(g-2)$ anomaly and other SM tensions in particle physics implying LFV effects [19–23]. We note that neutrino oscillations provide clear experimental evidence for LFV; however, for the charged lepton sector these effects are strongly suppressed. Therefore, in order to probe LFV phenomena one may address a new light vector field that violates charged lepton flavor at tree level. To be more specific, in the present paper we discuss the examination of a dark photon portal that can be relevant for LFV lepton decays and LFV processes at fixed-target experiments.

In the case of a dark photon, which can acquire mass via the Stueckelberg mechanism, the Lagrangian of its interaction with DM can be written as follows [15]:

$$\mathcal{L}'_{\rm DS} = -\frac{1}{4}A'_{\mu\nu}A'^{\mu\nu} + \frac{m^2_{A'}}{2}A'_\mu A'^\mu + \bar{\chi}(i\not{D}_\chi - m_\chi)\chi - \frac{1}{2\xi}(\partial_\mu A'^\mu)^2 + \frac{1}{2}\partial_\mu\sigma\partial^\mu\sigma - \xi\frac{m^2_{A'}}{2}\sigma^2, \quad (1)$$

where $m_{A'}$ is the mass of the dark photon, χ is a Dirac dark matter field, σ is the singlet Stueckelberg field, and ξ is the gauge-fixing parameter. The interaction of the dark photon A'_μ with charged leptons ψ_i can include both diagonal and nondiagonal couplings,

$$\mathcal{L}_{A'\psi} = \sum_{i,k=e,\mu,\tau} A'_\mu\bar{\psi}_i\gamma^\mu(g^V_{ik} + g^A_{ik}\gamma_5)\psi_k, \quad (2)$$

*zhevlakov@theor.jinr.ru
†kirpich@ms2.inr.ac.ru
‡valeri.lyubovitskij@uni-tuebingen.de

where g^V_{ik} and g^A_{ik} are the vector and axial-vector dimensionless couplings, respectively. Such couplings naturally arise in the familon scenarios [14,15] that imply an ultraviolet completion of the models. The bounds on leptophilic nondiagonal ($i \neq k$) dark photon couplings in Eq. (2) were derived explicitly in Refs. [14,15] from anomalous $(g-2)$ magnetic moments of charged leptons and the experimental constraints on rare $l_i \to \gamma l_k$ and $l_i \to 3l_k$ decays. It is worth noticing that diagonal couplings ($i = k$) in Eq. (2) may induce kinetic mixing between the SM photon and dark photon at the one-loop level [24]. (For a recent review on the corresponding constraints see, e.g., Ref. [6] and references therein.)

The paper is organized as follows. In Sec. II we discuss the contribution of the dark photon with nondiagonal lepton vertices to the anomalous magnetic moment of leptons. In Sec. III we briefly discuss two-body LFV decays involving a sub-GeV vector in the final state, $l_i \to l_f + A'$. In Sec. IV we derive the limits for nondiagonal coupling of the dark photon from fixed-target experiments. Finally, in Sec. V we present our bounds on the dark photon nondiagonal couplings with charged leptons and discuss search prospects for the LFV conversions $eN \to \mu NA'$, $\mu N \to eNA'$, $eN \to \tau NA'$, and $\mu N \to \tau NA'$ at fixed-target facilities.

II. LEPTON $(g-2)$ TENSIONS

The anomalous magnetic moments of both the muon and electron are the quantities that can be used to constrain the parameters of new physics models. In particular, the current discrepancies in $(g-2)$ between experimental measurements and theoretical predictions for the electron and muon in the framework of the SM are

$$\Delta a_\mu = (2.51 \pm 0.59) \times 10^{-9} \qquad [1], \tag{3}$$

$$|\Delta a_e| = (4.8 \pm 3.0) \times 10^{-13} \qquad [25]. \tag{4}$$

Here we use the difference between the theoretical and experimental values for $(g-2)$ for the muon based on the theoretical analysis of [1]. Now, the discrepancy in the value of the muon $(g-2)$ is due to the new data on the two-pion contribution to the hadronic vacuum polarization (HVP) from the CMD-3 Collaboration [26], new measurements of $(g-2)$ from the Muon $g-2$ experiment at Fermilab [27], and new theoretical discussions about the value of the HVP term [28–30]. In the BSM framework, the deviation in the magnitudes of the muon and electron $(g-2)$ can be potentially explained by the sub-GeV boson feebly interacting with leptons [31,32], which implies keeping nonzero diagonal couplings ($g^{A,V}_{ii} \neq 0$) and the vanishing of nondiagonal terms ($g^{A,V}_{ik} \equiv 0$). The precision of the measurements of the tau lepton anomalous magnetic moment is significantly worse, due the lack of experimental data on the short-lived tau [33,34]. For completeness, we refer Ref. [1] for the current status of the $(g-2)$ muon puzzle which use only SM calculation.

For the case of finite nondiagonal couplings ($g^{A,V}_{ik} \neq 0$) and vanishing couplings ($g^{V,A}_{ii} \equiv 0$), the typical contribution of a massive neutral dark vector boson to $(g-2)$ was calculated explicitly in Ref. [15]. In Fig. 1 we show the corresponding one-loop diagram. These quantities are given by one-dimensional integrals over the Feynman parameter:

$$\delta a^V_l = \frac{(g^V_{lf})^2}{4\pi^2} y_l \int_0^1 dx \frac{1-x}{\Delta(x, y_A, y_l)} \left[x(2 - y_l(1+x)) + \frac{(1-y_l)^2}{2y_A^2}(1 + y_l x)(1-x) \right], \tag{5}$$

$$\delta a^A_l = -\frac{(g^A_{lf})^2}{4\pi^2} y_l \int_0^1 dx \frac{1-x}{\Delta(x, y_A, y_l)} \left[x(2 + y_l(1+x)) + \frac{(1+y_l)^2}{2y_A^2}(1 - y_l x)(1-x) \right], \tag{6}$$

where $y_l = m_l/m_f$, $y_A = m_{A'}/m_f$, $\Delta(x,a,b) = a^2 x + (1-x)(1-b^2 x)$, m_l is the mass of external lepton, and m_f is the mass of the internal lepton in loop. In Fig. 2 we show the typical bounds on the nondiagonal coupling $g^V_{\mu e}$ from $(g-2)_e$ using a set of the ratios $g^A_{\mu e}/g^V_{\mu e}$. Similar bounds can be obtained from the $(g-2)_\mu$ discrepancy for $g^V_{\mu\tau}$ (see details in Ref. [15]).

The most stringent constraint on $g^V_{\mu e}$ implies $g^A_{\mu e} \ll 10^{-8}$, since the typical contributions of vector and axial-vector mediators have opposite signs in Eqs. (5) and (6) and thus the contribution of the vector field is maximal. For the benchmark ratio $g^V_{\mu e} \simeq g^A_{\mu e}$, the vector and axial-vector terms almost compensate each other at $m_{A'} \lesssim 2m_\mu$, which leads to a weakening of the limit on $g^V_{\mu e}$. Remarkably, there

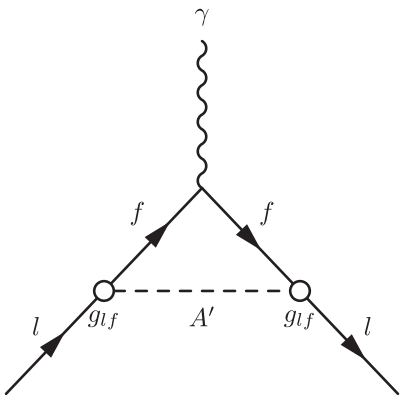

FIG. 1. Diagrams describing the contributions of the dark photon A' to the anomalous magnetic moments δa_l of the leptons with taking into account flavor nondiagonal ($l \neq f$) couplings, where $l, f = e, \mu, \tau$.

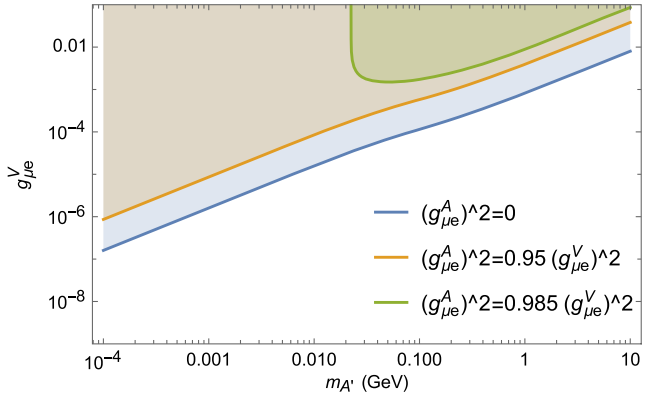

FIG. 2. Bounds for a nondiagonal coupling $g^V_{\mu e}$ from $(g-2)_e$ at different ratios between the axial-vector coupling $g^A_{\mu e}$ and vector coupling $g^V_{\mu e}$ of dark photon interactions with the muon and electron.

is a typical sensitivity mass threshold at $m_{A'} \gtrsim 2m_\mu$ for the benchmark ratio $g^A_{\mu e}/g^V_{\mu e} \simeq 1$.

III. INVISIBLE LEPTON DECAY MODE

If a dark photon with nondiagonal LFV couplings to muons (tau) and electrons (muon) is relatively light, i.e., $m_i \gtrsim m_{A'} + m_f$, then the decays $\mu \to e + \text{inv}$, $\tau \to e + \text{inv}$, and $\tau \to \mu + \text{inv}$ are kinematically allowed, where we imply the invisible decay of the dark photon in the final state $A' \to \chi\bar{\chi}$. In addition, the typical invisible charged LFV decays are searched for in the processes with lepton flavor conversion accompanied by the production of a neutrino-antineutrino pair [35,36]. It is worth noticing that the fixed-target experiments with missing energy/momenta technique can be a suitable using as tool to search for LFV signal with creation of dark particles.

The strongest bounds on the nondiagonal couplings of the dark photon with leptons for the area of $m_{A'} < 2m_e$ were obtained from experimental searches for the decays $\tau \to \mu + \text{inv}$ and $\tau \to e + \text{inv}$ by the ARGUS Collaboration [36] and from recent data from the Belle-II Collaboration [37]. We use the Particle Data Group data [34] to constrain the nondiagonal dark photon-lepton couplings $g^{V,A}_{\tau e}$ and $g^{V,A}_{\tau\mu}$. The bounds for axionlike particles were obtained in Ref. [38]. For $\mu \to e + \text{inv}$ decay we can use the limit obtained by the TWIST Collaboration [35], which predicts a branching ratio of up to 5.8×10^{-5}. Using this constraint, we show exclusion plots in Figs. 8 and 9.

The decay widths of such rare charged LFV decays $l_i \to l_f + A'$ in the vector and axial-vector cases are defined as

$$\Gamma(l_i \to l_f + A')_{V/A} = \frac{3(g^{V/A}_{if})^2 m_i}{8\pi} \lambda^{1/2}(y_i^2, y_f^2, 1) \times \left[(y_i \mp y_f)^2 - 1 + \frac{y_i^2}{3} \lambda(y_i^2, y_f^2, 1) \right], \quad (7)$$

where $y_i = m_i/m_{A'}$, $y_f = m_f/m_{A'}$, and $\lambda(x,y,z) = x^2 + y^2 + z^2 - 2xy - 2xz - 2yz$ is the Källen kinematical triangle function.

It is important to note that this decay depends only on nondiagonal coupling, while other LFV lepton decays such as $l_i \to l_f + \gamma$ or $l_i \to 3l_f$ have a dependence on the product of diagonal and nondiagonal couplings. An analysis of the parameter space of the dark photon was done in Ref. [39], where implication of the charged LFV two-body decay was noted as important bound.

IV. FIXED-TARGET EXPERIMENTS

Fixed-target experiments are very useful and crucial tests of the physics of feebly interacting particles and make up one-third of the experimental base for searches and analyses for DM [40] or hidden sectors. In this section, we study dark photon emission reactions with a change of lepton flavor.

In the framework of the benchmark scenario (2), stringent limits can be established from the missing energy/momenta experiments by the analysis of the $l_i + N \to l_f + N + A'$ process. In particular, we discuss the potential for fixed-target experiments with lepton beams, such as NA64$_e$ [32,41–45], LDMX [46–50], NA64$_\mu$ [51–54], and M^3 [55,56], which can be used to probe the invisible signatures associated with process of lepton flavor violation with missing energy. Missing energy signals can be evidence of dark photon emission that involves LFV processes. The analysis of final lepton states can give information about specific LFV channels of lepton conversion with dark photon emission.

The existing (NA64$_e$ [32,41–45] and NA64$_\mu$ [51–54]) and future experiments (LDMX [46–50] and M^3 [55,56]) are noted by us due to a possibility to use missing energy/momentum technique. NA64$_e$ and LDMX use electron beams that collide with active lead and aluminium targets, respectively. NA64$_\mu$ and M^3 use muon beams, and M^3 will use a tungsten target. We collect the main parameters of the fixed-target experiments NA64$_e$, NA64$_\mu$, M^3, and LDMX in Table I.

It is worth noticing that an analysis of LFV with dark matter emission at fixed-target experiments was done for the scalar case. In this respect, Refs. [8,57,58] examined the invisible scalar portal scenarios. The possibility of $e-\tau$ and $\mu-\tau$ conversion in deep-inelastic lepton scattering off nuclei was proposed and studied in detail in Ref. [59] based on the assumption of a local four-fermion lepton-quark interaction. Besides, we want to note a huge research work in study of lepton conversion on nucleons which was made in Refs. [60–63].

A. Signal of lepton conversion

Based on the setup of search in the missing energy experiment, we consider the reaction of a lepton scattering off the nucleus target, as shown in Fig. 3. We propose that

TABLE I. Parameters of the fixed-target experiments NA64$_e$, NA64$_\mu$, M^3, and LDMX: parameters of target (A, Z), first radiation length X_0, effective thickness of the target (L_T), energy of scattering beam and current (started) and planned accumulate of leptons on target, $x_{\min}$ characterizing a window of search.

	e-conversion	μ-conversion	$A(Z)$	E (GeV)	ρ (g cm^{-3})	X_0 (cm)	L_T (cm)	$x_{\min}$	LoT (projected LoT)
NA64$_e$:	$eN \to NA'\mu(\tau)$	$\cdots$	207 (82)	100	11.34	0.56	0.56	0.5	3.3×10^{11} (5×10^{12})
NA64$_\mu$:	$\cdots$	$\mu N \to NA'e(\tau)$	207 (82)	160	11.34	0.56	22.5	0.5	10^{10} (10^{13})
M^3:	$\cdots$	$\mu N \to NA'e(\tau)$	184 (74)	15	19.3	0.35	17.5	0.4	10^{10} (10^{13})
LDMX:	$eN \to NA'\mu(\tau)$	$\cdots$	27 (13)	16	2.7	8.9	3.56	0.7	10^{16} (10^{18})

the dark photon has a longer lifetime than the time of flight inside the detector or the dominant decay mode into dark matter. The invisible two-body decay width of the dark photon A' into a $\bar{\chi}\chi$ pair is given by

$$\Gamma_{A'\to\bar{\chi}\chi} = \frac{g_D^2}{12\pi} m_{A'}(1+2y_\chi^2)(1-4y_\chi^2)^{1/2}, \tag{8}$$

where g_D is the coupling between the dark photon and dark fermions and $y_\chi = m_\chi/m_{A'}$.

For our calculation, we use the Weizsäcker-Williams (WW) approximation [64,65]. In this case, the interaction signal of incoming leptons (e,μ) with the atomic target can be effectively described through the Compton-like process with lepton conversion on virtual photons γ^*, i.e., via $l\gamma^* \to l'A'$. We also suppose that the target nucleus has a spin of $1/2$ and its coupling to photons is $ieZF(t)\gamma_\mu$, where $F(t)$ is an elastic form factor depending on $t = -q^2 > 0$ (nucleus transfer momentum squared) and Z is the charge of the nucleus. $F(t)$ has the form

$$F(t) = \frac{a^2 t}{(1+a^2 t)} \frac{1}{(1+t/d)}, \tag{9}$$

where $a = 111Z^{-1/3}/m_e$ and $d = 0.164A^{-2/3}$ GeV^2 are the screening and nucleus size parameters, respectively [66]. These nuclear form factor parameters include the mass of electron m_e and atomic mass number A.

The differential cross section for the $2 \to 3$ process, presented in Fig. 3, in the framework of the WW approximation is given by

$$\frac{d\sigma_{lZ\to l'ZA'}}{d(pk)d(k\mathcal{P}_i)} \simeq \frac{\alpha\gamma_Z}{\pi(p'\mathcal{P}_i)} \cdot \left.\frac{d\sigma_{l\gamma^*\to l'A'}}{d(pk)}\right|_{t=t_{\min}}, \tag{10}$$

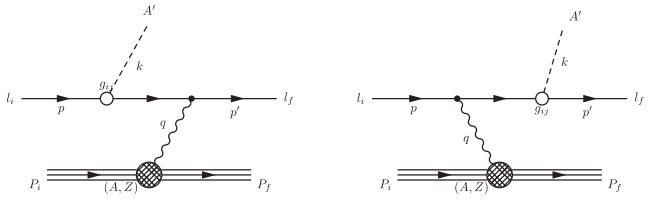

FIG. 3. Lowest-order diagrams describing LFV emission of a dark photon A' in lepton scattering on a fixed atomic target.

where $t_{\min}$ is the minimal momentum transfer [provided in Eq. (19)], $\alpha \simeq 1/137.036$ is the fine-structure constant, and γ_Z is the effective photon flux from the nucleus defined as

$$\gamma_Z = Z^2 \int_{t_{\min}}^{t_{\max}} dt \frac{t - t_{\min}}{t^2} F^2(t), \tag{11}$$

where $\mathcal{P}_i$ are initial and finale momenta of nuclear, p, p', and k are the momenta of initial leptons, final leptons, and the dark photon (see definition in Fig. 3), and $t_{\max}$ and $t_{\min}$ are kinematic bounds obtained from the energy-conserving δ function in the Lorentz-invariant phase space (for details, see Ref. [67]).

By using such an approximation, we can calculate the typical number of missing energy events for experiments with a lepton beam impinging on a fixed target,

$$N_{A'} \simeq \mathrm{LoT} \cdot \frac{\rho N_A}{A} L_T \int_{x_{\min}}^{x_{\max}} dx \frac{d\sigma_{2\to3}}{dx}(E), \tag{12}$$

where N_A is Avogadro's number, LoT is the number of leptons accumulated on target, ρ is the target density, L_T is the effective interaction length of the lepton in the target, $d\sigma_{2\to3}/dx$ is the differential cross section of the lepton conversion $lN \to l'NA'$, E is the initial lepton beam energy, $x = E_{A'}/E$ is the energy fraction that the dark photon carries away, $x_{\min} = E_{\mathrm{cut}}/E$ and $x_{\max} \simeq 1$ are the minimal and maximal fraction of dark photon energy, respectively, for the experimental setup, and E_{cut} is a detector missing energy cut that is determined by the specific facility. The typical parameters of the experiments can be found in Refs. [32,41–44,46–50,53–56,68]. For muon beam experiments (NA64$_\mu$ and M^3) we use MoT to denote the number of muons on target, and for electron beam experiments (NA64$_e$ and LDMX) we use EoT to denote the number of electrons on target.

B. Cross section

The amplitude of the $2 \to 2$ process $l_i(p) + \gamma(q) \to l_f(p') + A'(k)$ is given by

$$M^{2\to2} = ie\epsilon^{\mu}_{\lambda}\epsilon^{*\alpha}_{\lambda'}\bar{u}_f(p',s')\left[\gamma_\mu\frac{p-k+m_i}{\tilde{u}}(\gamma_\alpha g^V_{if}+\gamma_5\gamma_\alpha g^A_{if}) + (\gamma_\alpha g^V_{if}+\gamma_5\gamma_\alpha g^A_{if})\frac{p'+k+m_f}{\tilde{s}}\gamma_\mu\right]u_i(p,s), \quad (13)$$

where we used the notation $p = \gamma^\mu p_\mu$, g^V_{if} and g^A_{if} are the nondiagonal couplings of interaction of the dark photon with leptons, ϵ is the polarization vector of the photon or dark photon, and m_i and m_f are the masses of the initial and final leptons. The sums over polarizations are given by

$$\sum_{\lambda}\epsilon^{\mu}_{\lambda}\epsilon^{*\nu}_{\lambda} = -g^{\mu\nu} \quad (14)$$

for visible photons and

$$\sum_{\lambda'}\epsilon^{\mu}_{\lambda'}\epsilon^{*\nu}_{\lambda'} = -g^{\mu\nu} + \frac{k^\mu k^\nu}{m^2_{A'}}, \quad (15)$$

for massive dark photons. In the case of visible photons, we use the $\xi \to \infty$ gauge and omit ghost-field contributions.

After averaging and summing over the spins of leptons and polarizations of vector bosons, one gets the matrix element squared,

$$\overline{|M^{2\to2}|^2} = \frac{1}{4}\sum_{s,s'}\sum_{\lambda,\lambda'}|M^{2\to2}|^2 = e^2(g^V_{if})^2A^{2\to2}_V + e^2(g^A_{if})^2A^{2\to2}_A. \quad (16)$$

In our calculation, we use the so-called modified Mandelstam variables,

$$\begin{aligned}\tilde{s} &= (p'+k)^2 - m_f^2 = 2(p'k) + m^2_{A'},\\ \tilde{u} &= (p-k)^2 - m_i^2 = -2(pk) + m^2_{A'},\\ t_2 &= (p'-p)^2 = -2(p'p) + m_i^2 + m_f^2,\\ t &= q^2,\end{aligned} \quad (17)$$

which satisfy the condition $\tilde{s} + t_2 + \tilde{u} = m^2_{A'}$.

When considering the process, the initial lepton energy is much greater than the masses of $m_{A'}$ and m_f. In this case, we can use the WW approximation and propose with high reliability that the final states of the lepton and dark photon are highly collinear. In the small-angle approximation (which means that $t = t_{\min}$), we imply that $\mathbf{q}$ and $\mathbf{V} = \mathbf{k} - \mathbf{p}$ are collinear [65,67] and the modified Mandelstam variables are given by

$$\begin{aligned}U = -\tilde{u} &\approx E^2x\theta^2 + m_i^2x + \frac{1-x}{x}m^2_{A'},\\ \tilde{s} &\approx \frac{U + (m_f^2 - m_i^2)x}{1-x},\end{aligned} \quad (18)$$

$$\begin{aligned}t_2 &\approx -\frac{x}{1-x}(U + (m_f^2 - m_i^2)) + m^2_{A'},\\ t_{\min} &\approx \frac{(\tilde{s} + (m_f^2 - m_i^2))^2}{4E^2}.\end{aligned} \quad (19)$$

Note that if we set $m_i = m_f$, then we reproduce the formulas presented in Refs. [66,67].

The double differential cross section can be presented in the form

$$\frac{d\sigma_{2\to3}}{dx\,d\,\cos\theta_{A'}} \simeq \frac{\alpha\gamma_Z}{\pi(1-x)}\cdot E^2x\beta_{A'}I_{\tilde{s}}\cdot\frac{d\sigma_{2\to2}}{d(pk)}, \quad (20)$$

where $\beta_{A'} = (1 - m^2_{A'}/(xE)^2)^{1/2}$ is the velocity of the dark photon in the laboratory frame, $I_{\tilde{s}} = \tilde{s}^2/(\tilde{s} + (m_f^2 - m_i^2))^2\beta^{-1}_{m_i}$, and $\beta_{m_i} = \sqrt{1 - m_i^2/E^2}$. The full analytical expression for the effective photon flux χ was presented in Ref. [53]. It is known that the elastic form factor $G_{\rm el}(t)$ is proportional to $\propto Z^2$. An inelastic form factor is suppressed by a factor Z, i.e., $G_{\rm inel}(t) \propto Z$, and therefore for the heavy target nuclei $Z \propto \mathcal{O}(100)$ one can safely ignore it in calculations.

The differential cross section [67] can be rewritten as

$$\frac{d\sigma^{V,A}_{2\to2}}{d(pk)} = 2\frac{d\sigma}{dt_2} = \frac{\overline{|M^{2\to2}|^2}}{8\pi\tilde{s}^2} = (g^{V,A}_{if})^2\frac{\alpha}{\tilde{s}^2}A^{2\to2}_{V,A}, \quad (21)$$

where the vector and axial-vector parts of the amplitudes squared can be written, respectively, as

$$\begin{aligned}A^{2\to2}_{V,t=t_{\min}} \approx \frac{1}{\tilde{s}^2U^2m^2_{A'}}&(\tilde{s}(\tilde{s}-U)^2U(m_i-m_f)^2 + (2\tilde{s}U(\tilde{s}^2+U^2) + (\tilde{s}^2+U^2)m_i^4 + 6(\tilde{s}-U)^2m_i^3m_f\\ &+ 2(\tilde{s}^3 + 2\tilde{s}^2U + U^3)m_f^2 + (\tilde{s}^2+U^2)m_f^4 + 6m_im_f(U-\tilde{s})(2\tilde{s}U + (U-\tilde{s})m_f^2)\\ &- 2m_i^2(\tilde{s}^3 + 2\tilde{s}U^2 + U^3 + (3\tilde{s}^2 - 4\tilde{s}U + 3U^2)m_f^2))m^2_{A'} + 2(2\tilde{s}U(U-\tilde{s}) + U(-3\tilde{s}+2U)m_i^2\\ &+ 6\tilde{s}Um_im_f + \tilde{s}(2\tilde{s}-3U)m_f^2)m^4_{A'} + 4\tilde{s}Um^6_{A'}),\end{aligned} \quad (22)$$

$$A^{2\to 2}_{A,t=t_{\min}} \approx \frac{1}{\tilde{s}^2U^2m^2_{A'}}(\tilde{s}(\tilde{s}-U)^2U(m_i+m_f)^2+(2\tilde{s}U(\tilde{s}^2+U^2)+(\tilde{s}^2+U^2)m_i^4-6(\tilde{s}-U)^2m_i^3m_f$$
$$+2(\tilde{s}^3+2\tilde{s}^2U+U^3)m_f^2+(\tilde{s}^2+U^2)m_f^4+6(U-\tilde{s})m_im_f(-2\tilde{s}U+(\tilde{s}-U)m_f^2)$$
$$-2m_i^2(\tilde{s}^3+2\tilde{s}U^2+U^3+(3\tilde{s}^2-4\tilde{s}U+3U^2)m_f^2))m^2_{A'}-2(2\tilde{s}(\tilde{s}-U)U+(3\tilde{s}-2U)Um_i^2$$
$$+6\tilde{s}Um_im_f+\tilde{s}(3U-2\tilde{s})m_f^2)m^4_{A'}+4\tilde{s}Um^6_{A'}). \quad (23)$$

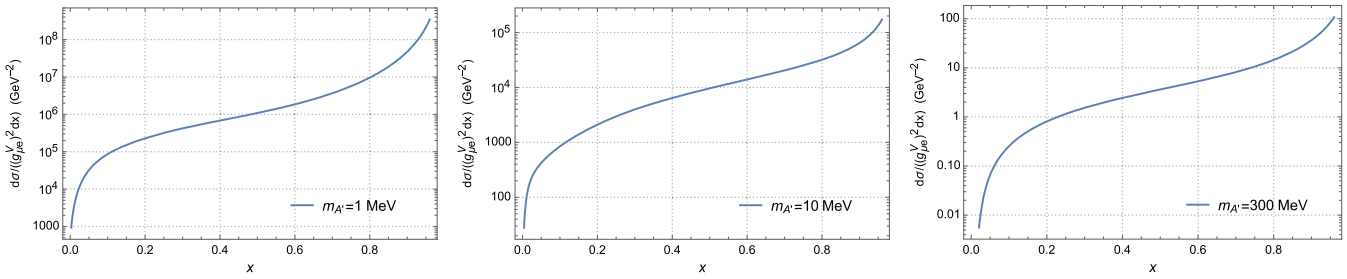

FIG. 4. Differential cross section $d\sigma/((g^V_{\mu e})^2dx)$ for the process of electron-to-muon conversion in the case of a vector nondiagonal coupling of the dark photon with a lepton for the NA64$_e$ experiment with different dark photon masses and the typical electron beam energy $E = 100$ GeV.

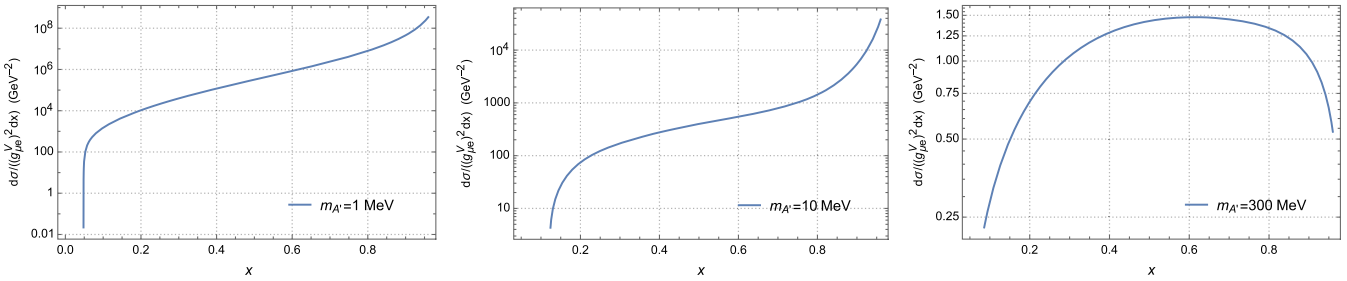

FIG. 5. Differential cross section $d\sigma/((g^V_{\mu e})^2dx)$ for the process of muon-to-electron conversion in the case of a vector nondiagonal coupling of the dark photon with a lepton for the NA64$_\mu$ experiment with dark photon different masses and the typical muon beam energy $E = 160$ GeV.

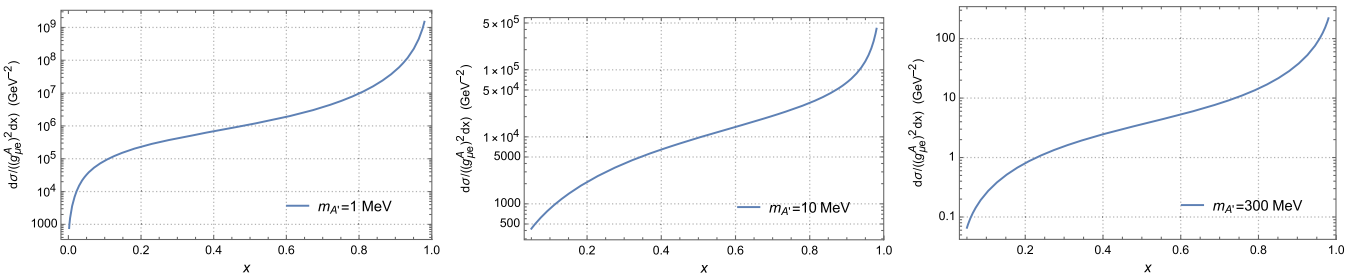

FIG. 6. Same as in Fig. 4 but for an axial-vector field.

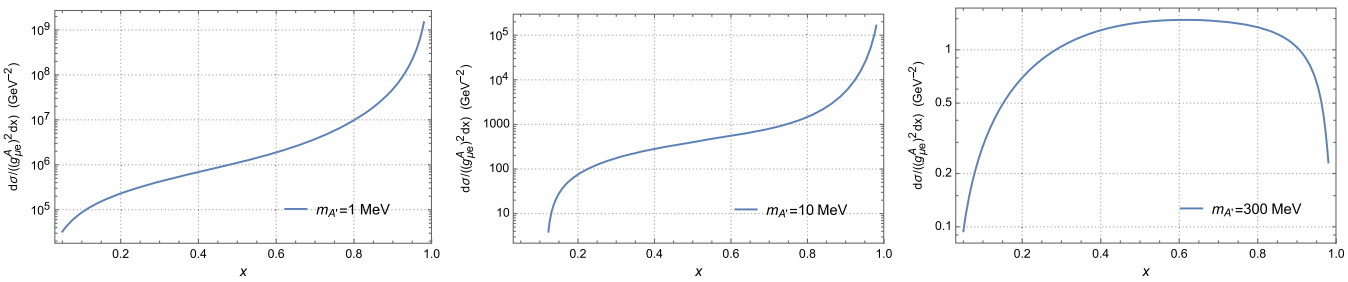

FIG. 7. Same as in Fig. 5 but for an axial-vector field.

In our calculations we use the FeynCalc package [69–71] and the following assumptions to exploit the WW approximation: (i) the cross section for processes with $m_i > m_f$ is evaluated by taking into account the nonzero emission angle of the final particle [72], $\theta_{\min} \simeq [(m_i^2 + m_{A'}^2 - m_f^2)/(|\mathbf{k}||\mathbf{p}|)]^{1/2}$, and (ii) the maximal typical angle of dark photon emission is set to $\theta_{\max} \simeq 0.1$. As a result, the integration over the angle $\theta_{A'}$ is performed in the range $\theta_{\min} \lesssim \theta_{A'} \lesssim \theta_{\max}$.

In order to illustrate our results for the differential cross sections $d\sigma/dx$ we make a comparison between different combinations of initial and final states of leptons, as shown in Figs. 4–7. For the case of equal masses of initial and final leptons, we reproduce the numerical results presented in Refs. [31,67]. These cross sections $d\sigma/dx$ are calculated by using Eqs. (20) and (21), implying the lepton beam energy and target characteristics of the NA64$_e$ and NA64$_\mu$ experiments. One can see the similar shapes of the vector and axial-vector dark photons in the case of $e \to \mu$ conversion cross sections at $m_{A'} \simeq 1$ MeV. For larger masses, $m_{A'} \gtrsim 300$ MeV, the differential spectra of vector and axial-vector dark photons almost coincide. For the case of $\mu \to e$ conversion cross sections, one can see sharp peaks at $x \simeq 1$ for the relatively light dark photon $m_{A'} \lesssim 10$ MeV. The corresponding peaks are mitigated for heavy masses $m_{A'} \gtrsim 300$ MeV.

V. RESULTS AND DISCUSSION

In this section, we derive the bounds on nondiagonal $g_{ik}^{V,A}$ couplings of the dark photon with leptons from the lepton scattering experiments at fixed targets, which implies LFV conversion $lN \to l'NA'$ followed by the invisible decay of the dark photon with $\mathrm{Br}(A' \to \chi\bar{\chi}) \simeq 1$. We set the diagonal couplings to be $g_{ii}^{V,A} \equiv 0$ throughout the analysis.

Our results for the exclusion limits on vector and axial-vector couplings are presented in Figs. 8 and 9 at 90% CL, implying zero observed signal events and background free case for the fixed-target experiments, we are assumption that theoretical uncertainty is negligible, $N_{A'} \lesssim 2.3$. In particular, the analysis reveals [73] that the electron beam mode NA64$_e$ is background free for EoT $\simeq \mathcal{O}(1) \times 10^{12}$. In addition, for our analysis of the muon beam mode at NA64$_\mu$ we rely on the studies in [54,57,74] which implies the background suppression at the level of $\lesssim \mathcal{O}(1) \times 10^{-13}$ per muon for the LFV process due to the emission of a spin-0 boson ϕ, i.e., in the reaction $lN \to l'N\phi$. Furthermore, for the background suppression of both the LDMX and M^3 facilities we rely on the explicit analysis of [75] and [55], respectively, for the reactions without LFV, $lN \to lNA'$, implying conservatively that the background rejections would be the same for the LFV process, $lN \to l'NA'$.

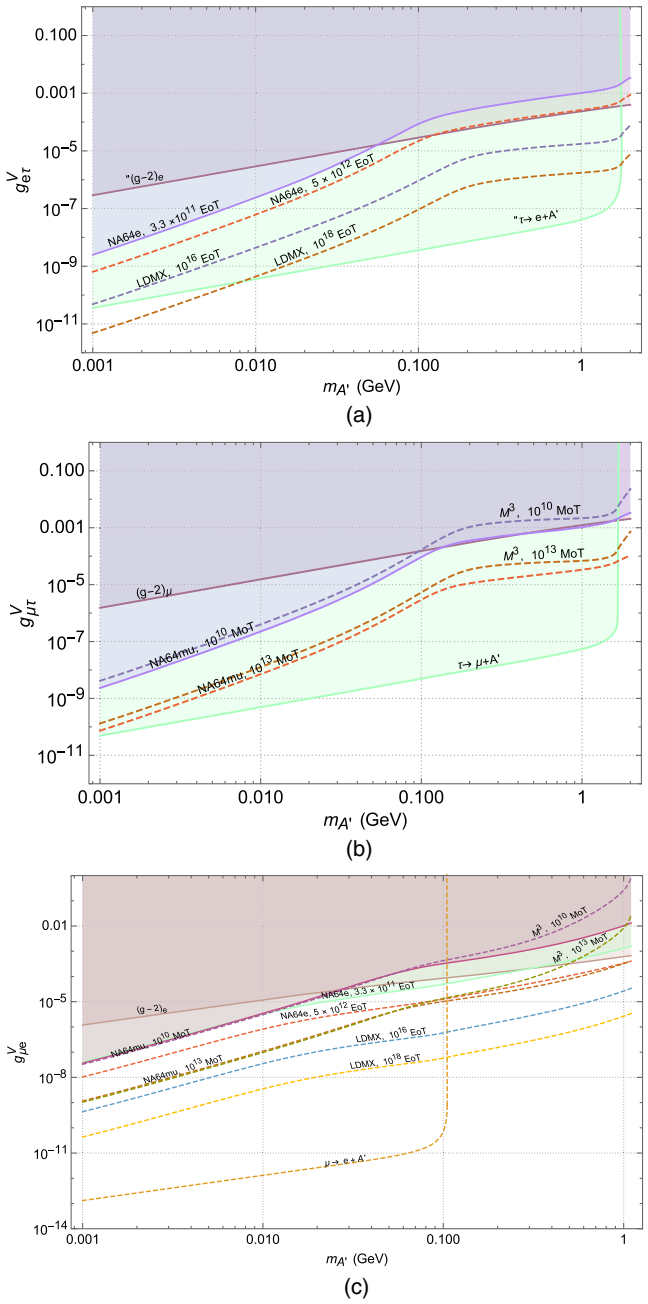

FIG. 8. Bounds on vector nondiagonal coupling of a dark photon with leptons using characteristics of the running and proposed fixed-target experiments NA64$_e$, NA64$_\mu$, LDMX, and M^3. Bounds from the $g-2$ of leptons and invisible lepton LFV decay $l_i \to l_f + A'$ are included. (a): bounds for $g_{e\tau}^V$. (b): bounds for $g_{\mu\tau}^V$. (c): bounds for $g_{\mu e}^V$.

To search a channel of LFV conversion in $lN \to l'NA'$ process is needed to search a signal with missing energy and single different flavor lepton. For the benchmark conversion $e(\mu)N \to \tau NA'$ and the typical dark photon mass range $m_{A'} \lesssim 1$ GeV, the existing fixed-target experiments (NA64$_e$ and NA64$_\mu$) cannot reach the bound on

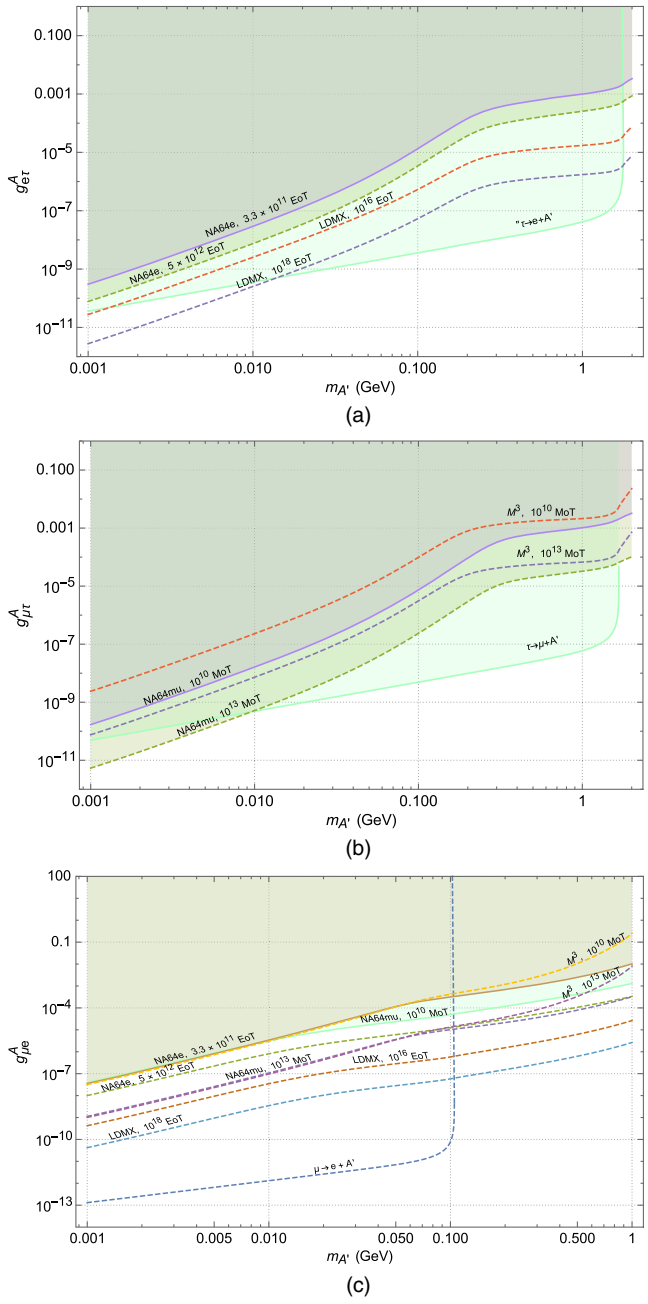

FIG. 9. Bounds on axial-vector nondiagonal coupling of a dark photon with leptons using characteristics of the running and proposed fixed-target experiments NA64$_e$, NA64$_\mu$, LDMX, and M^3. Bounds from the $g-2$ of leptons and invisible lepton LFV decay $l_i \to l_f + A'$ are included. (a): bounds for $g^A_{e\tau}$. (b): bounds for $g^A_{\mu\tau}$. (c): bounds for $g^A_{\mu e}$.

$\tau \to e(\mu)A'$ from the ARGUS experiment [36] for both vector $[g^V_{e\tau}(g^V_{\mu\tau})]$ and axial-vector $[g^A_{e\tau}(g^A_{\mu\tau})]$ couplings. For the considered benchmark scenarios, the most stringent constraints on the couplings $g^V_{e\tau} \lesssim 10^{-11}$ and $g^A_{e\tau} \lesssim 10^{-11}$ at $m_{A'} \lesssim 1$ MeV are expected from the projected statistics (EoT $= 10^{18}$) of the LDMX experiment. However, for the typical mass range $m_{A'} \gtrsim 100$ MeV the LDMX experiment is able to set the constraint at the level of $g^{V,A}_{\mu e} \lesssim 10^{-7}$. Remarkably, for the typical mass range $m_{A'} \gtrsim m_\tau \simeq 1.7$ GeV, the LDMX facility can set the bounds at $g^{V,A}_{e\tau} \lesssim 10^{-5} - 10^{-4}$. For the accumulated statistics of NA64$_e$ at the level of EoT $\simeq 3.3 \times 10^{11}$, the corresponding experiment provides the bound $g^A_{e\tau} \lesssim 5 \times 10^{-3}$ for the mass threshold range $m_{A'} \gtrsim 1.7$ GeV. In addition, the NA64$_e$ experiment also rules out the typical regions $g^V_{\mu e} \lesssim 10^{-4}$ for 100 MeV $\lesssim m_{A'} \lesssim 300$ MeV and $g^A_{\mu e} \lesssim 10^{-3} - 10^{-2}$ for 100 MeV $\lesssim m_{A'} \lesssim 1$ GeV.

The NA64$_\mu$ fixed-target experiment can provide a more stringent limit than the M^3 facility. Moreover, the expected reaches of the LDMX and NA64$_\mu$ experiments at the dark photon masses $m_{A'} \lesssim 1$ MeV can be comparable with the current bounds from two-body LFV lepton decay, $\tau \to \mu(e)A'$. In addition, the current limits from missing energy data of the NA64$_e$ and NA64$_\mu$ experiments are comparable with the bounds from $(g-2)_{e,\mu}$ tensions of leptons. We note that for the projected statistics MoT $\simeq 10^{13}$, both NA64$_\mu$ and M^3 can rule out the typical region $g^{V,A}_{\mu\tau} \lesssim 10^{-4}$–$10^{-3}$ for the relatively heavy dark photon masses $m_{A'} \gtrsim 1.7$ GeV. Moreover, for the mass range 100 MeV $\lesssim m_{A'} \lesssim 1$ GeV the NA64$_\mu$ experiment is able to set the constraint $g^{A,V}_{\mu e} \lesssim 10^{-5}$ for MoT $\simeq 10^{13}$.

Finally, we would like to note that one can probe the resonant production of dark photons in the LFV reaction of a muon scattering off atomic electrons $\mu^+ e^- \to A' \to \chi\bar{\chi}$ at both the NA64$_\mu$ and M^3 muon beam fixed-target experiments. However, this analysis is beyond the scope of the present paper and we plan to study it in the future.

ACKNOWLEDGMENTS

The work of A. S. Zh. on exclusion limit calculations for the fixed-target experiments is supported by the Russian Science Foundation (Grant No. RSF 23-22-00041). The work of A. S. Zh. on exclusion limit calculations from $(g-2)$ tension is supported by the Foundation for the Advancement of Theoretical Physics and Mathematics "BASIS." The work of D. V. K. on signal yield calculations for the $e \to \mu$ conversion at NA64$_e$ experiments is supported by the Russian Science Foundation (Grant No. RSF 21-12-00379). The work of V. E. L. was funded by ANID PIA/APOYO AFB220003 (Chile) (Chile), FONDECYT (Chile) under Grant No. 1230160, and ANID-Millennium Program-ICN2019_044 (Chile).

[1] T. Aoyama *et al.*, Phys. Rep. **887**, 1 (2020).
[2] E. Aprile *et al.* (XENON Collaboration), Phys. Rev. D **102**, 072004 (2020).
[3] T. Aaltonen *et al.* (CDF Collaboration), Science **376**, 170 (2022).
[4] A. A. Aguilar-Arevalo *et al.* (MiniBooNE Collaboration), Phys. Rev. D **103**, 052002 (2021).
[5] A. J. Krasznahorkay *et al.*, Phys. Rev. Lett. **116**, 042501 (2016).
[6] C. Antel *et al.*, Eur. Phys. J. C **83**, 1122 (2023).
[7] G. Arcadi, A. Djouadi, and M. Raidal, Phys. Rep. **842**, 1 (2020).
[8] S. N. Gninenko and N. V. Krasnikov, Phys. Rev. D **106**, 015003 (2022).
[9] H. Davoudiasl, R. Marcarelli, and E. T. Neil, J. High Energy Phys. 02 (2023) 071.
[10] I. V. Voronchikhin and D. V. Kirpichnikov, Phys. Rev. D **107**, 115034 (2023).
[11] I. V. Voronchikhin and D. V. Kirpichnikov, Phys. Rev. D **106**, 115041 (2022).
[12] Y.-J. Kang and H. M. Lee, Eur. Phys. J. C **80**, 602 (2020).
[13] F. Fortuna, P. Roig, and J. Wudka, J. High Energy Phys. 02 (2021) 223.
[14] A. J. Buras, A. Crivellin, F. Kirk, C. A. Manzari, and M. Montull, J. High Energy Phys. 06 (2021) 068.
[15] A. Kachanovich, S. Kovalenko, S. Kuleshov, V. E. Lyubovitskij, and A. S. Zhevlakov, Phys. Rev. D **105**, 075004 (2022).
[16] M. Escudero, N. Rius, and V. Sanz, J. High Energy Phys. 02 (2017) 045.
[17] Y. Nomura and J. Thaler, Phys. Rev. D **79**, 075008 (2009).
[18] V. E. Lyubovitskij, A. S. Zhevlakov, A. Kachanovich, and S. Kuleshov, Phys. Rev. D **107**, 055006 (2023).
[19] G. Arcadi, C. P. Ferreira, F. Goertz, M. M. Guzzo, F. S. Queiroz, and A. C. O. Santos, Phys. Rev. D **97**, 075022 (2018).
[20] C. Han, M. L. López-Ibáñez, A. Melis, O. Vives, and J. M. Yang, Phys. Rev. D **103**, 035028 (2021).
[21] D. Aloni, A. Dery, C. Frugiuele, and Y. Nir, J. High Energy Phys. 11 (2017) 109.
[22] Z. Poh and S. Raby, Phys. Rev. D **96**, 015032 (2017).
[23] T. Araki, K. Asai, H. Otono, T. Shimomura, and Y. Takubo, J. High Energy Phys. 01 (2023) 145.
[24] B. Holdom, Phys. Lett. B **166**, 196 (1986).
[25] L. Morel, Z. Yao, P. Cladé, and S. Guellati-Khélifa, Nature (London) **588**, 61 (2020).
[26] F. V. Ignatov *et al.* (CMD-3 Collaboration), arXiv: 2302.08834.
[27] D. P. Aguillard *et al.* (Muon g-2 Collaboration), Phys. Rev. Lett. **131**, 161802 (2023).
[28] T. Blum *et al.* (RBC and UKQCD Collaborations), Phys. Rev. D **108**, 054507 (2023).
[29] M. Davier, A. Hoecker, A. M. Lutz, B. Malaescu, and Z. Zhang, arXiv:2312.02053.
[30] S. Borsanyi *et al.*, Nature (London) **593**, 51 (2021).
[31] D. V. Kirpichnikov, V. E. Lyubovitskij, and A. S. Zhevlakov, Phys. Rev. D **102**, 095024 (2020).
[32] Y. M. Andreev *et al.* (NA64 Collaboration), Phys. Rev. Lett. **126**, 211802 (2021).
[33] S. Eidelman and M. Passera, Mod. Phys. Lett. A **22**, 159 (2007).
[34] R. L. Workman *et al.* (Particle Data Group), Prog. Theor. Exp. Phys. **2022**, 083C01 (2022).
[35] R. Bayes *et al.* (TWIST Collaboration), Phys. Rev. D **91**, 052020 (2015).
[36] H. Albrecht *et al.* (ARGUS Collaboration), Z. Phys. C **68**, 25 (1995).
[37] I. Adachi *et al.* (Belle-II Collaboration), Phys. Rev. Lett. **130**, 181803 (2023).
[38] M. Bauer, M. Neubert, S. Renner, M. Schnubel, and A. Thamm, Phys. Rev. Lett. **124**, 211803 (2020).
[39] J. Heeck, Phys. Lett. B **758**, 101 (2016).
[40] G. Lanfranchi, M. Pospelov, and P. Schuster, Annu. Rev. Nucl. Part. Sci. **71**, 279 (2021).
[41] S. N. Gninenko, D. V. Kirpichnikov, M. M. Kirsanov, and N. V. Krasnikov, Phys. Lett. B **782**, 406 (2018).
[42] S. N. Gninenko, D. V. Kirpichnikov, M. M. Kirsanov, and N. V. Krasnikov, Phys. Lett. B **796**, 117 (2019).
[43] D. Banerjee *et al.*, Phys. Rev. Lett. **123**, 121801 (2019).
[44] Y. M. Andreev *et al.*, Phys. Rev. D **104**, L091701 (2021).
[45] N. Arefyeva, S. Gninenko, D. Gorbunov, and D. Kirpichnikov, Phys. Rev. D **106**, 035029 (2022).
[46] A. Berlin, N. Blinov, G. Krnjaic, P. Schuster, and N. Toro, Phys. Rev. D **99**, 075001 (2019).
[47] T. Åkesson *et al.* (LDMX Collaboration), arXiv: 1808.05219.
[48] A. M. Ankowski, A. Friedland, S. W. Li, O. Moreno, P. Schuster, N. Toro, and N. Tran, Phys. Rev. D **101**, 053004 (2020).
[49] P. Schuster, N. Toro, and K. Zhou, Phys. Rev. D **105**, 035036 (2022).
[50] T. Åkesson *et al.*, arXiv:2203.08192.
[51] S. N. Gninenko, N. V. Krasnikov, and V. A. Matveev, Phys. Rev. D **91**, 095015 (2015).
[52] S. N. Gninenko and N. V. Krasnikov, Phys. Lett. B **783**, 24 (2018).
[53] D. V. Kirpichnikov, H. Sieber, L. M. Bueno, P. Crivelli, and M. M. Kirsanov, Phys. Rev. D **104**, 076012 (2021).
[54] H. Sieber, D. Banerjee, P. Crivelli, E. Depero, S. N. Gninenko, D. V. Kirpichnikov, M. M. Kirsanov, V. Poliakov, and L. Molina Bueno, Phys. Rev. D **105**, 052006 (2022).
[55] Y. Kahn, G. Krnjaic, N. Tran, and A. Whitbeck, J. High Energy Phys. 09 (2018) 153.
[56] R. Capdevilla, D. Curtin, Y. Kahn, and G. Krnjaic, J. High Energy Phys. 04 (2022) 129.
[57] B. Radics, L. Molina-Bueno, L. Fields, H. Sieber, and P. Crivelli, Eur. Phys. J. C **83**, 775 (2023).
[58] Y. Ema, Z. Liu, K.-F. Lyu, and M. Pospelov, J. High Energy Phys. 02 (2023) 135.
[59] S. Gninenko, S. Kovalenko, S. Kuleshov, V. E. Lyubovitskij, and A. S. Zhevlakov, Phys. Rev. D **98**, 015007 (2018).
[60] M. Gonzalez, T. Gutsche, J. C. Helo, S. Kovalenko, V. E. Lyubovitskij, and I. Schmidt, Phys. Rev. D **87**, 096020 (2013).
[61] A. Faessler, T. Gutsche, S. Kovalenko, V. E. Lyubovitskij, and I. Schmidt, Phys. Rev. D **72**, 075006 (2005).
[62] A. Faessler, T. Gutsche, S. Kovalenko, V. E. Lyubovitskij, I. Schmidt, and F. Simkovic, Phys. Rev. D **70**, 055008 (2004).

[63] A. Faessler, T. Gutsche, S. Kovalenko, V. E. Lyubovitskij, I. Schmidt, and F. Simkovic, Phys. Lett. B **590**, 57 (2004).
[64] V. M. Budnev, I. F. Ginzburg, G. V. Meledin, and V. G. Serbo, Phys. Rep. **15**, 181 (1975).
[65] Y.-S. Tsai, Rev. Mod. Phys. **46**, 815 (1974); **49**, 421(E) (1977).
[66] J. D. Bjorken, R. Essig, P. Schuster, and N. Toro, Phys. Rev. D **80**, 075018 (2009).
[67] Y.-S. Liu and G. A. Miller, Phys. Rev. D **96**, 016004 (2017).
[68] A. S. Zhevlakov, D. V. Kirpichnikov, and V. E. Lyubovitskij, Phys. Rev. D **106**, 035018 (2022).
[69] V. Shtabovenko, R. Mertig, and F. Orellana, Comput. Phys. Commun. **207**, 432 (2016).
[70] V. Shtabovenko, Comput. Phys. Commun. **218**, 48 (2017).
[71] V. Shtabovenko, R. Mertig, and F. Orellana, Comput. Phys. Commun. **256**, 107478 (2020).
[72] E. Byckling and K. Kajantie, *Particle Kinematics* (University of Jyvaskyla, Jyvaskyla, Finland, 1971).
[73] Y. M. Andreev *et al.* (NA64 Collaboration), Phys. Rev. Lett. **131**, 161801 (2023).
[74] H. Sieber, D. V. Kirpichnikov, I. V. Voronchikhin, P. Crivelli, S. N. Gninenko, M. M. Kirsanov, N. V. Krasnikov, L. Molina-Bueno, and S. K. Sekatskii, Phys. Rev. D **108**, 056018 (2023).
[75] T. Åkesson *et al.* (LDMX Collaboration), J. High Energy Phys. 04 (2020) 003.